

by projecting onto a temperature-density diagram. None of these equations represents well the density dependence of the present system. Figure 1 shows the comparison of the coexistence curves for four compositions on the temperature-density diagram between measured values and calculated values by the Peng-Robinson equation with  $k_{ij} = 0$  as a typical example. The effect of introducing  $k_{ij}$  was contradictory for each composition as mentioned above, and it was not efficient to improve description of liquid density. We might conclude that the cubic equations of state would not be good enough to reproduce the density values measured particularly for the liquid state.

#### Acknowledgment

T. Kamimura, Y. Watanabe, and M. Fukasawa have provided valuable assistance in the experiments.

Registry No. R 13B1, 75-63-8; R 114, 76-14-2.

#### Literature Cited

- (1) Takaishi, Y.; Kagawa, N.; Uematsu, M.; Watanabe, K. *Proc. Symp. Thermophys. Prop. 8th* 1982, 2, 387.
- (2) Hasegawa, N.; Uematsu, M.; Watanabe, K. *J. Chem. Eng. Data* 1985, 30, 32.
- (3) Takaishi, Y.; Uematsu, M.; Watanabe, K. *Bull. Jpn. Soc. Mech. Eng.* 1982, 25, 944.
- (4) Okano, T.; Uematsu, M.; Watanabe, K. *Int. J. Thermophys.* 1987, 8, 217.
- (5) Soave, G. *Chem. Eng. Sci.* 1972, 27, 1197.
- (6) Peng, D.; Robinson, D. B. *Ind. Eng. Chem. Fundam.* 1976, 15, 59.
- (7) Patel, N. C.; Teja, A. S. *Chem. Eng. Sci.* 1982, 37, 463.

Received for review September 10, 1986. Accepted August 24, 1987. We are greatly indebted to Du Pont-Mitsui Fluorochemicals Co., Ltd., Tokyo, for kindly furnishing the samples of R 13B1 and R 114. We are also grateful to the National Research Laboratory of Metrology, Ibaraki, Japan, for their calibration of the thermometer.

**Supplementary Material Available:** Complete form of Table I including the experimental data in the two-phase region (22 pages). Ordering information is given on any current masthead page.

## Measurements of the Vapor-Liquid Coexistence Curve for the R 13B1 + R 114 System in the Critical Region

Y. Higashi,\*† Y. Kabata, M. Uematsu, and K. Watanabe

Department of Mechanical Engineering, Kelo University, Yokohama 223, Japan

**Measurements of the vapor-liquid coexistence curve in the critical region for the refrigerant mixture of bromotrifluoromethane (CBrF<sub>3</sub>, R 13B1) and 1,2-dichloro-1,1,2,2-tetrafluoroethane (CCl<sub>2</sub>CCl<sub>2</sub>F<sub>2</sub>, R 114) were made by visual observation of the disappearance of the meniscus at the vapor-liquid interface within an optical cell. Eighteen saturated-vapor densities and 21 saturated-liquid densities for four different compositions of 25, 50, 70, and 80 wt % R 13B1 between 345 and 406 K were obtained in the range of densities 356-1166 kg/m<sup>3</sup>. The experimental error of temperature, density, and mass fraction was estimated within ±15 mK, ±0.5%, and ±0.05%, respectively. On the basis of these measurements, the critical curve of the R 13B1 + R 114 system is determined and compared with several predictive methods. In addition, new correlation so as to represent the composition dependence of the critical parameters for the R 13B1 + R 114 system is proposed.**

#### Introduction

Nonazeotropic refrigerant mixtures, so-called NARBs (nonazeotropic refrigerant blends), of two or three kinds of halogenated hydrocarbons have recently been of interest as prospective working fluids in the reversed Rankine cycle systems. For example, Cooper et al. (1) showed that the R 13B1 (bromotrifluoromethane, CBrF<sub>3</sub>) + R 152a (1,1-difluoroethane, CH<sub>3</sub>CHF<sub>2</sub>) system was an attractive choice to replace R 22 (chlorodifluoromethane, CHClF<sub>2</sub>) in an air-to-air heat pump with an accumulator and capillary tube expander, and that the R 13B1 + R 152a system supplied approximately 40% more heating capacity than R 22 in a 7-kW heat pump. Moreover, the low-temperature medical freezer using the ternary refrig-

erant mixture of the R 502 (azeotropic mixture of R 22 + R 115 (CCl<sub>2</sub>CF<sub>3</sub>, chloropentafluoroethane) + R 12 (dichlorodifluoromethane, CCl<sub>2</sub>F<sub>2</sub>) system as well as the ternary refrigerant mixture of the R 21 (dichlorofluoromethane, CHCl<sub>2</sub>F) + R 13B1 + R 14 (tetrafluoromethane, CF<sub>4</sub>) system as a working fluid is commercialized (2).

We have been carrying out investigations on the thermophysical properties of several refrigerant mixtures. Some of the results were published: measurements of the vapor-liquid coexistence curve in the critical region and the critical curve for the R 12 + R 22 system (3) and the R 22 + R 114 system (4), the PVTx measurements of the R 12 + R 22 system (5-7), the R 22 + R 114 (1,2-dichloro-1,1,2,2-tetrafluoroethane, CCl<sub>2</sub>CCl<sub>2</sub>F<sub>2</sub>) system (8), and the R 13B1 + R 114 system (9). In the present paper, measurements of the vapor-liquid coexistence curve and the critical curve for the R 13B1 + R 114 system in the critical region are reported, and the assessment of the predictive methods of the critical parameters is also discussed on the basis of the experimental results of the critical parameters for refrigerant mixtures. The correlations of the composition dependence of the critical parameters are proposed.

#### Experimental Section

The vapor-liquid coexistence curve in the critical region and the critical point for a certain composition of binary refrigerant mixtures were measured by observing the meniscus disappearance. The experimental apparatus used and procedures were described in detail in previous publications (10, 11). The apparatus was composed of an optical cell, an expansion vessel, and a supplying vessel. In order to measure the saturation temperature successively for a series of densities along the coexistence curve, we introduced an expansion technique (10) throughout the measurements. The optical cell was connected with the expansion vessel to repeat the expansion procedures of the sample fluid from the optical cell to the ex-

\* Present address: Department of Mechanical Engineering, Iwaki Meisei University, Iwaki, Fukushima 970, Japan.

**Table I. Experimental Results along the Coexistence Curve for the R 13B1 + R 114 System<sup>a</sup>**

| <i>T</i> , K        | $\rho$ , kg/m <sup>3</sup> | <i>T</i> , K        | $\rho$ , kg/m <sup>3</sup> |
|---------------------|----------------------------|---------------------|----------------------------|
| 25.00 wt % R 13B1   |                            |                     |                            |
| 404.79 <sub>0</sub> | 363.8 ± 1.7                | 401.03 <sub>1</sub> | 697.8 ± 1.1                |
| 405.24 <sub>9</sub> | 446.4 ± 1.6*               | 400.03 <sub>6</sub> | 763.0 ± 1.2                |
| 404.81 <sub>0</sub> | 488.1 ± 1.8*               | 395.53 <sub>6</sub> | 888.8 ± 0.7                |
| 403.96 <sub>6</sub> | 568.5 ± 1.6*               | 390.44 <sub>8</sub> | 972.1 ± 0.8                |
| 403.31 <sub>3</sub> | 621.6 ± 1.7*               |                     |                            |
| 50.00 wt % R 13B1   |                            |                     |                            |
| 389.15 <sub>4</sub> | 356.6 ± 1.7                | 384.07 <sub>6</sub> | 746.9 ± 0.6*               |
| 389.12 <sub>1</sub> | 476.7 ± 1.3                | 381.79 <sub>0</sub> | 872.4 ± 0.7                |
| 387.93 <sub>5</sub> | 557.7 ± 1.6*               | 372.54 <sub>4</sub> | 1026.8 ± 0.8               |
| 386.10 <sub>9</sub> | 656.6 ± 1.8*               |                     |                            |
| 70.00 wt % R 13B1   |                            |                     |                            |
| 373.83 <sub>1</sub> | 388.1 ± 1.8                | 368.75 <sub>0</sub> | 686.6 ± 0.5*               |
| 373.50 <sub>7</sub> | 439.2 ± 1.2                | 367.95 <sub>9</sub> | 744.5 ± 1.2*               |
| 371.41 <sub>0</sub> | 519.6 ± 1.9                | 366.82 <sub>6</sub> | 812.2 ± 1.3                |
| 370.38 <sub>9</sub> | 606.6 ± 1.7*               | 363.27 <sub>1</sub> | 948.4 ± 0.8                |
| 369.25 <sub>2</sub> | 661.8 ± 1.9*               | 359.14 <sub>1</sub> | 1034.7 ± 0.8               |
| 80.00 wt % R 13B1   |                            |                     |                            |
| 361.13 <sub>5</sub> | 472.6 ± 2.2                | 359.16 <sub>6</sub> | 797.6 ± 0.6*               |
| 362.28 <sub>5</sub> | 543.9 ± 2.0                | 358.85 <sub>0</sub> | 812.6 ± 1.3*               |
| 361.91 <sub>4</sub> | 600.5 ± 2.2                | 357.28 <sub>0</sub> | 897.2 ± 1.4                |
| 360.11 <sub>7</sub> | 706.2 ± 2.0*               | 353.38 <sub>1</sub> | 1028.1 ± 0.8               |
| 359.87 <sub>2</sub> | 716.7 ± 0.6*               | 351.76 <sub>6</sub> | 1055.1 ± 0.8               |
| 359.53 <sub>5</sub> | 730.2 ± 0.6*               | 345.40 <sub>3</sub> | 1165.2 ± 0.9               |
| 359.65 <sub>0</sub> | 772.9 ± 0.6*               |                     |                            |

<sup>a</sup> Values with an asterisk were measured by observing the critical opalescence.

pansion vessel after the measurements of a saturation temperature. The supplying vessel was connected to both the optical cell and the expansion vessel, which allowed the sample in the supplying vessel to be supplied to the optical cell after the completion of a single series of expansion procedures. Careful attention was paid to the expansion procedure so as not to change the sample composition and also to homogenize the sample density after the expansion procedure. The sample density in the optical cell can be calculated from the mass of the sample and the inner volumes of the three vessels used. With this method it is unavoidable that the experimental uncertainty in the density measurements becomes larger proportionally to the total number of expansion procedures. Therefore, we restricted the number of expansion procedures to maintain the uncertainty of density measurements within 0.5%. The prescribed quantity of each pure component, which was weighed in advance, was prepared separately and they were charged one by one into the supplying vessel immersed in the liquefied nitrogen. The mass fraction of the sample mixture thus provided was determined to be the ratio of the mass of each component to that of the mixture with an uncertainty of no greater than 0.05%. The temperature measurements were conducted with a 25- $\Omega$  platinum resistance thermometer (Chino, Model R800-1) calibrated with a precision of 5 mK on the IPTS-68 at the National Research Laboratory of Metrology, Ibaraki, Japan, with an aid of a thermometer bridge (Tinsley, Type 5840). The uncertainty in temperature measurements was estimated to be  $\pm 15$  mK including the precision of the thermometer used, the fluctuation of the temperature controlled, and an individual difference in the determination of the meniscus-disappearance temperature.

The purity of each component used was either 99.965 or 99.990 wt % R 13B1 and either 99.94 or 99.98 wt % R 114 being an isomeric blend of 95% CClF<sub>2</sub>CClF<sub>2</sub> + 5% CCl<sub>2</sub>FCF<sub>3</sub>.

## Results

The experimental temperature–density data along the coexistence curve for four different compositions of 25, 50, 70, and

**Table II. Critical Parameters for the R 13B1 + R 114 System<sup>a</sup>**

| compos of R 13B1 |                  | <i>T</i> <sub>c</sub> , K | $\rho_c$ , kg/m <sup>3</sup> | <i>P</i> <sub>c</sub> , MPa |
|------------------|------------------|---------------------------|------------------------------|-----------------------------|
| <i>w</i> , wt %  | <i>x</i> , mol % |                           |                              |                             |
| 0                | 0                | 418.78 ± 0.02             | 576 ± 3                      | 3.252 ± 0.004               |
| 25.00            | 27.67            | 403.39 ± 0.10             | 615 ± 10                     | 3.76 ± 0.03                 |
| 50.00            | 53.44            | 386.23 ± 0.10             | 650 ± 10                     | 4.16 ± 0.03                 |
| 70.00            | 72.81            | 368.92 ± 0.05             | 678 ± 7                      | 4.24 ± 0.03                 |
| 80.00            | 82.12            | 360.07 ± 0.02             | 708 ± 4                      | 4.23 ± 0.03                 |
| 100              | 100              | 340.08 ± 0.01             | 764 ± 3                      | 3.956 ± 0.002               |

<sup>a</sup> Critical parameters for 0 and 100 wt % R 13B1 are quoted from ref 12 and 11, respectively.

80 wt % R 13B1 are given in Table I. The results of measurements for both pure components were published previously (11, 12). Nine, seven, ten, and thirteen measurements for 25, 50, 70, and 80 wt % R 13B1, respectively, cover the temperature range from 345 to 406 K and the density range from 356 to 1166 kg/m<sup>3</sup>. The measured results with an asterisk in Table I were obtained when the meniscus disappeared and the critical opalescence was observed simultaneously. The behavior of the meniscus and the intensity of the critical opalescence for the R 13B1 + R 114 system were observed similarly as pure components (11, 12) except those in the vicinity of the critical point. In this region, the critical opalescence at the vapor phase was observed as intensely as that at the liquid phase, while the meniscus ascended or descended very slightly. With the approach of temperature to the critical, the meniscus became indistinguishable at the center level of the optical cell and a fog band was formed. Then, after the temperature was kept constant within a fluctuation of 5 mK for a period of 2–5 h, it was confirmed that this fog band had disappeared. Similar phenomena were observed in the case of R 114 (12) and also in the case of R 22 + R 114 system (4).

The critical temperature *T*<sub>c</sub> and the critical density  $\rho_c$  of the respective compositions for the present R 13B1 + R 114 system were determined by analyzing the present measurements listed in Table I, taking into consideration the disappearing meniscus level and intensity of the critical opalescence. The critical pressure *P*<sub>c</sub> of the respective compositions was determined graphically with an aid of the *PVTx* measurements by Hosotani et al. (9) for the R 13B1 + R 114 system. The critical parameters thus obtained for R 13B1 + R 114 system are given in Table II including those for pure components which were published previously (11, 12). The mass fraction of respective compositions for the mixtures measured was converted into the mole fraction by using the molar mass of 148.910 g/mol for R 13B1 and that of 170.92 g/mol for R 114. The uncertainties of the critical parameters listed in Table II, on the whole, become larger than those for the mixtures measured previously, i.e., the R 12 + R 22 system (3) and the R 22 + R 114 system (4). This depends on the shape of the vapor–liquid coexistence curve near the critical point. The shape of the vapor–liquid coexistence curve for the present system is so skewed that temperature gradient against density along the vapor–liquid coexistence curve becomes greater than those of the R 12 + R 22 system (3) and the R 22 + R 114 system (4). Taking account of this temperature gradient, the larger uncertainties of the critical temperature than those for the other two systems have been estimated.

## Discussion

The density of the maximum temperature along the coexistence curve for respective compositions, which is the density at the so-called "maxcondentherm point", for the R 13B1 + R 114 system shifts from the critical density of respective compositions to the lower density by about 200–300 kg/m<sup>3</sup>. The temperatures at the maxcondentherm point are higher than the

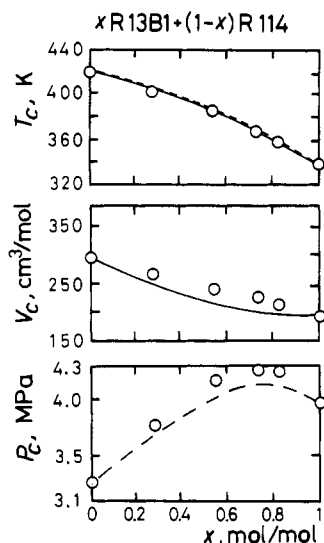


**Figure 1.** Comparisons of composition dependence of the critical parameters between the experimental results [O] and the empirical predictive methods; Chueh–Prausnitz [—], Li [---], Kreglewski–Kay [---].

critical temperature of the respective compositions determined by visual observations by about 1.8–4.6 K. These temperature differences are much larger than those of the other two systems we measured: not larger than 0.2 K for the R 12 + R 22 system (3), and 0.8–1.5 K for the R 22 + R 114 system (4). The critical temperature difference between pure components is 16, 50, and 79 K for the R 12 + R 22 system, for the R 22 + R 114 system, and for the R 13B1 + R 114 system, respectively. The shape of the vapor–liquid coexistence curves for respective compositions of the present R 13B1 + R 114 system is skewed most heavily among the three systems we measured.

The composition dependence of the critical parameters listed in Table II were compared with empirical predictive methods recommended by Reid et al. (14), i.e., that for the critical temperature by Li (15), that for the critical temperature and the critical molar volume by Chueh and Prausnitz (16), and that for the critical pressure by Kreglewski and Kay (17), respectively. The results of comparison is shown in Figure 1. With respect to the critical temperature, the results of two predictive methods by Li and by Chueh–Prausnitz are in good agreement with the present results, although those for the R 12 + R 22 system and the R 22 + R 114 system are much higher than the experimental results by about 0.5–2.5%. The results of the predictive method by Chueh–Prausnitz for the critical molar volume is lower than the present results by about 5–15%. The Chueh–Prausnitz method predicts well this property for the R 12 + R 22 system (3), but it gives lower values both for the R 22 + R 114 system (4) and for the present system. With respect to the critical pressure, the result of the predictive method by Kreglewski–Kay is lower than the present results by about 1–3%. The prediction by Kreglewski–Kay for the R 22 + R 114 system (4) shows in good agreement with the experimental results, although the predictions for both the R 12 + R 22 system (3) and the present system give lower values.

Figure 2 shows comparison of the composition dependence of the critical parameters listed in Table II with those calculated by two cubic equations of state: Soave–Redlich–Kwong (SRK) equation (18) and Peng–Robinson (PR) equation (19). The binary interaction parameter in each equation,  $k_{12}$ , was determined to minimize the average deviation from present results of the critical temperature for respective compositions. The values of  $k_{12}$  are 0.0057 for the SRK equation and 0.084 for the PR equation. The PR equation predicts well the composition dependence of both the critical molar volume and the critical

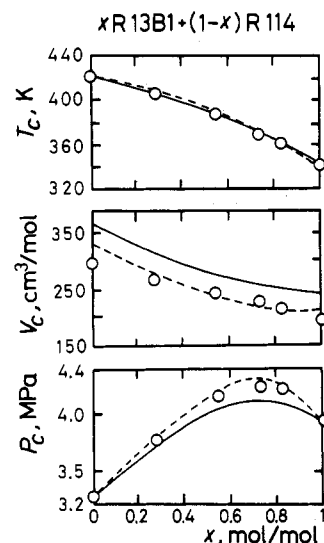


**Figure 2.** Comparisons of composition dependence of the critical parameters between the experimental results [O] and the values calculated from cubic equations of state; SRK equation with  $k_{12} = 0.0057$  [—]; PR equation with  $k_{12} = 0.084$  [---].

pressure, although the PR equation deviates from the experimental data of the critical molar volume of both pure components by 11% and 10% for R 13B1 and R 114, respectively. The SRK equation does not reproduce the composition dependence of the critical molar volume as in the case of the R 22 + R 114 system (4). As for the composition dependence of the critical pressure, the prediction by the SRK equation is lower than the present results by about 1–3%.

The composition dependence of the critical parameters for the R 13B1 + R 114 system was correlated to eq 1–3, whose functional forms were originally proposed by Chueh and Prausnitz (16), for the critical temperature, critical pressure, and critical molar volume, respectively, based on the present results.

$$T_{cm} = \theta_1 T_{c1} + \theta_2 T_{c2} + 2\theta_1\theta_2\Delta_T \quad (1)$$

$$P_{cm} = \theta_1 P_{c1} + \theta_2 P_{c2} + 2\theta_1\theta_2\Delta_P \quad (2)$$

$$V_{cm} = \theta_1 V_{c1} + \theta_2 V_{c2} + 2\theta_1\theta_2\Delta_V \quad (3)$$

Here,  $T_{cm}$ ,  $P_{cm}$ , and  $V_{cm}$  denote the critical temperature of mixture, the critical pressure of mixture, and the critical molar volume of mixture, respectively.  $\theta$  denotes a surface fraction given by eq 4 and subscript 1 and 2 correspond to each component of mixture.  $\Delta_T$ ,  $\Delta_P$ , and  $\Delta_V$  are adjustable parameters for the critical temperature, critical pressure, and critical molar volume, respectively.

$$\theta_i = x_i V_{ci}^{2/3} / \sum_j x_j V_{cj}^{2/3} \quad (4)$$

Here,  $x$  denotes mole fraction. The eq 1–3 with  $\Delta_T = 6.9$  K,  $\Delta_P = 1.2$  MPa, and  $\Delta_V = -5.2$  cm<sup>3</sup>/mol reproduce the present results best with an average deviation of 0.061%, 0.54%, and 0.82% for the critical temperature, critical pressure, and critical molar volume, respectively.

#### Acknowledgment

The assistance of Hajime Hasebe, who made these elaborate computations and experiments with the present authors, is gratefully acknowledged.

#### Glossary

|          |                                   |
|----------|-----------------------------------|
| $k_{12}$ | binary interaction parameter      |
| $P$      | pressure, MPa                     |
| $P_c$    | critical pressure, MPa            |
| $P_{cm}$ | critical pressure of mixture, MPa |

|            |  |
|------------|--|
| $T$        | temperature, K   |
| $T_c$      | critical temperature, K                                |
| $T_{cm}$   | critical temperature of mixture, K                     |
| $V$        | molar volume, cm <sup>3</sup> /mol                     |
| $V_c$      | critical molar volume, cm <sup>3</sup> /mol            |
| $V_{cm}$   | critical molar volume of mixture, cm <sup>3</sup> /mol |
| $x$        | mole fraction of R 13B1, mol/mol                       |
| $w$        | mass fraction of R 13B1, kg/kg                         |
| $\Delta_p$ | adjustable parameter in eq 2, MPa                      |
| $\Delta_T$ | adjustable parameter in eq 1, K                        |
| $\Delta_V$ | adjustable parameter in eq 3, cm <sup>3</sup> /mol     |
| $\theta$   | surface fraction                                       |
| $\rho$     | density, kg/m <sup>3</sup>                             |
| $\rho_c$   | critical density, kg/m <sup>3</sup>                    |

Registry No. R 13B1, 75-63-8; R 114, 76-14-2.

#### Literature Cited

- (1) Cooper, W. D.; Borchardt, H. J. *Proc. 15th Int. Congr. Refrig. Int. Inst. Refrig., Venice* 1979, 995.
- (2) Sanyo Electric Trading Co. Ltd. Technical Report, 1983.
- (3) Higashi, Y.; Okazaki, S.; Takaishi, Y.; Uematsu, M.; Watanabe, K. *J. Chem. Eng. Data* 1984, 29, 31.
- (4) Higashi, Y.; Uematsu, M.; Watanabe, K. *Int. J. Thermophys.* 1986, 7, 29.

- (5) Takaishi, Y.; Kagawa, N.; Uematsu, M.; Watanabe, K. *Proc. 8th Symp. Thermophys. Prop.* 1981, 2, 387.
- (6) Takaishi, Y.; Uematsu, M.; Watanabe, K. *Bull. JSME* 1982, 25, 944.
- (7) Takaishi, Y.; Kagawa, N.; Uematsu, M.; Watanabe, K. *Bull. JSME* 1984, 27, 1696.
- (8) Hasegawa, N.; Uematsu, M.; Watanabe, K. *J. Chem. Eng. Data* 1985, 30, 32.
- (9) Hosotani, S.; Maezawa, Y.; Uematsu, M.; Watanabe, K. *J. Chem. Eng. Data*, in press.
- (10) Okazaki, S.; Higashi, Y.; Takaishi, Y.; Uematsu, M.; Watanabe, K. *Rev. Sci. Instrum.* 1983, 54, 21.
- (11) Higashi, Y.; Uematsu, M.; Watanabe, K. *Bull. JSME* 1985, 28, 2660.
- (12) Higashi, Y.; Uematsu, M.; Watanabe, K. *Bull. JSME* 1985, 28, 2968.
- (13) Higashi, Y.; Ashizawa, M.; Kabata, Y.; Majima, T.; Uematsu, M.; Watanabe, K. *JSME Int. J.* 1987, 30, 1106.
- (14) Reid, R. C.; Prausnitz, J. M.; Sherwood, T. K. *The Properties of Gases and Liquids*, 3rd ed.; McGraw-Hill: New York, 1977.
- (15) Li, C. C. *Can. J. Chem. Eng.* 1971, 49, 709.
- (16) Chueh, P. L.; Prausnitz, J. M. *AIChE J.* 1967, 13, 1107.
- (17) Kreglewski, A.; Kay, W. B. *J. Phys. Chem.* 1969, 73, 3359.
- (18) Soave, G. *Chem. Eng. Sci.* 1972, 27, 1197.
- (19) Peng, D.; Robinson, D. B. *Ind. Eng. Chem., Fundam.* 1976, 15, 59.

Received for review March 16, 1987. Accepted September 16, 1987. We are greatly indebted to the National Research Laboratory of Metrology, Ibaraki, Japan, for the calibration of the thermometer, to Shin-etsu Chemicals Co., Ltd., Tokyo, for kindly furnishing the silicone oil, and also to Du Pont-Mitsui Fluorochemicals Co. Ltd., Tokyo, for kindly furnishing the sample. Financial support of the Grant-in-Aid for Scientific Research Fund in 1985 (Project No. 60790040) by the Ministry of Education, Science and Culture, Japan, to Y.H. is gratefully appreciated.

## Vapor-Liquid Equilibria for the Ammonia-Methanol-Water System

Hiroshi Inomata, Noboru Ikawa, Kunio Arai, and Shozaburo Saito\*

Department of Chemical Engineering, Tohoku University, Aramaki, Aoba, Sendai, Japan 980

Vapor-liquid equilibrium data are reported for the ammonia-water system at 60 °C and the ammonia-water system at 40 and 60 °C at pressures up to 2.5 MPa. Isobaric vapor-liquid equilibrium data are reported for the ammonia-methanol-water system at 2.0 MPa and at 60, 100, and 140 °C. A new apparatus was developed for these measurements and good agreement with available literature data of Kudo and Toriumi for the ammonia-methanol system could be obtained. Correlation of the data with the Patel-Teja equation of state and van der Waals random mixing rules failed to reproduce the curvature of the  $P$ - $x$  diagrams; however, mixing rules based on Wilson's local composition model could reproduce the detailed system behavior.

#### Introduction

To recover unreacted ammonia and methanol in the amine production process, it is necessary to separate these components from water. Distillation at atmospheric pressure is currently used for such separation; however, separation at high pressure might be suitable from the viewpoint of energy requirements because the reactor in the amine process is operated at high pressure and, in addition, the latent heat of vaporization at high pressure is smaller compared with that at low pressure.

A knowledge of the vapor-liquid equilibria for the mixtures consisting of ammonia, methanol, and water is essential for the design of such high-pressure separation processes. In this work, the vapor-liquid equilibria for the above-mentioned ternary systems was measured at high pressure and correlated with an equation of state.

#### Experimental Section

**Materials.** Methanol with purity 99.6% was obtained from Wako Pure Chemical Industries Ltd., and liquified ammonia was available in relatively high purity (99.97%) from Nippon Sanso Products. No secondary peaks could be detected from gas chromatographic analysis. Water was ion-exchanged and purified through distillation.

**Apparatus and Procedure.** A schematic diagram of the apparatus developed in this study is shown in Figure 1. This static-type apparatus, in which coexisting phases were continuously circulated, consisted of (1) a dual-windowed equilibrium cell; (2) a recycling system for each coexisting phase; and (3) a sampling and analyzing system. Each part of the apparatus was immersed in a constant temperature air bath controlled to an accuracy of better than  $\pm 1$  °C. Figure 2 shows the details of the 750 cm<sup>3</sup> internal volume equilibrium cell which was machined from 316 type stainless steel. A methanol-water mixture of known amount and composition was pumped into the evacuated equilibrium cell, 1, by a charging pump, 3. Ammonia was first transferred to the sample cylinder, 12, from the gas cylinder, 14, and then to the cell, 1. The desired pressure was obtained by controlling the vapor pressure of ammonia in the sample cylinder. Equilibrium was achieved by stirring with magnetic stirrer, 8, and recirculating of each phase with the magnetic pumps, 7. To avoid composition change by the condensation of the polar components during recirculation of the vapor phase, the temperature of the recirculation tubing was maintained at slightly higher (2-3 °C) than the equilibrium temperature, whereas the temperature for the liquid phase recirculation tubing was slightly lower (2-3 °C) than the equilibrium temperature to avoid vaporization of the liquid phase. The change of the cell temperature due to this temperature control of the recirculation tubings was determined to be negligible.